INTERNATIONAL ATOMIC ENERGY AGENCY
UNITED NATIONS EDUCATIONAL, SCIENTIFIC AND CULTURAL ORGANIZATION

INTERNATIONAL CENTRE FOR THEORETICAL PHYSICS
34100 TRIESTE (ITALY) - P.O.B. 586 - MIRAMARE - STRADA COSTIERA 11 - TELEPHONES: 224281/2/3/4/5/6
CABLE: CENTRATOM - TELEX 460392-I

SMR/113 - 8

AUTUMN COLLEGE

ON

THE TROPOSPHERE, STRATOSPHERE AND MESOSPHERE

10 September - 19 October 1984

HIGH-VORTICITY REGIONS IN ROTATING THERMALLY DRIVEN FLOWS

R. HIDE

Geophysical Fluid Dynamics Laboratory
Meteorological Office (21)
Bracknell
Berkshire RG12 2SZ
U.K.

-1-

Reproduced from the
METEOROLOGICAL MAGAZINE
Vol. 110, 1981, 335–344

551.511.2:551.511.3:523.45

High-vorticity regions in rotating thermally driven flows*

By R. Hide, F.R.S.
(Meteorological Office, Bracknell)

Summary

The regular and irregular non-axisymmetric flow regimes of thermal convection in a rotating fluid annulus subject to differential heating in the horizontal are characterized by the presence of upper-level jet streams, where intense concentrations of vorticity and high concomitant horizontal temperature gradients are found. The main features of the upper-level flow pattern can be interpreted by straightforward arguments based on general thermodynamic considerations and the requirement that the flow should be quasi-geostrophic nearly everywhere. Thus, when the distribution of applied heating and cooling is such that the corresponding gradient of the impressed radial temperature field has the same sign at all radii, the most conspicuous feature of the upper-level flow pattern in the regular non-axisymmetric regime is a single jet stream meandering in a wavy pattern between the bounding cylinders. When, however, the impressed radial temperature gradient changes sign near mid-radius (as in the case when heat is introduced throughout the body of the fluid and withdrawn at both side-walls), the corresponding upper-level flow consists of several closed eddies, each circulating 'anticyclonically' with the horizontal flow largely confined to a narrow jet stream at the periphery of each eddy. In some respects these stable closed eddies are dynamically similar to long-lived anticyclonic eddies (including the Great Red Spot) seen in Jupiter's atmosphere in the southern hemisphere. Previous work on stable baroclinic eddies is now being extended in various directions and supporting numerical work is also being carried out.

1. Introduction

The motion of a fluid that departs but little from solid body rotation with angular velocity Ω is usually geostrophic nearly everywhere, with the relative Eulerian velocity $\boldsymbol{u}$ (as measured in a frame of reference that rotates with angular velocity Ω relative to an inertial frame) satisfying

$$2\rho\Omega \times \boldsymbol{u} = -\nabla p + \rho\nabla V. \qquad \ldots \quad \ldots \quad \ldots \quad \ldots \quad (1)$$

* Invited paper presented at the joint International Union for Theoretical and Applied Mechanics/International Union for Geodesy and Geophysics symposium on *Intense Atmospheric Vortices*, 14–17 July 1981, European Centre for Medium-range Weather Forecasts, Shinfield Park, near Reading, England.

-2-

Here ρ denotes density, p denotes pressure and ∇V is the acceleration due to gravity and centripetal effects. Equation (1) is the leading approximation to the full equation of motion,

$$\rho\left(\frac{D\boldsymbol{u}}{Dt} + 2\Omega \times \boldsymbol{u} - \boldsymbol{r} \times \frac{d\Omega}{dt}\right) = -\nabla p + \rho\nabla V - \nabla \times (\nu\rho\nabla \times \boldsymbol{u}). \quad \ldots \quad \ldots \quad (2)$$

It is valid in regions where the Coriolis term $2\rho\Omega \times \boldsymbol{u}$ greatly exceeds the relative acceleration term $\rho D\boldsymbol{u}/Dt \equiv \rho(\partial\boldsymbol{u}/\partial t + \boldsymbol{u}.\nabla\boldsymbol{u})$ (where t denotes time), the precessional term $\rho\boldsymbol{r} \times d\Omega/dt$, the viscous term $\nabla \times (\nu\rho\nabla \times \boldsymbol{u})$ (where ν denotes kinematic viscosity) and any other term that must be added to equation (2) when further effects (e.g. magnetohydrodynamic forces) have to be taken into account.

Now equation (1) is lower in order than equation (2), so it cannot be solved under the complete set of boundary conditions. For this to be possible it is necessary to include every term in equation (2) in the analysis. It follows that the flow cannot be geostrophic everywhere; the system must exhibit boundary layers and detached shear layers where $\rho D\boldsymbol{u}/Dt + \nabla \times (\rho\nu\nabla \times \boldsymbol{u})$ is comparable in magnitude with $2\rho\Omega \times \boldsymbol{u}$. Within these highly ageostrophic regions the magnitude of the relative vorticity $\nabla \times \boldsymbol{u}$ can be comparable with or even exceed 2Ω. Many examples of such vorticity concentrations are found in laboratory systems and in nature. They are often associated with steep gradients of temperature (thermal fronts), as in the case of jet streams and western boundary currents found in atmospheres and oceans.

Jet streams are a pronounced feature of the non-axisymmetric flow regimes of thermal convection in a rotating fluid annulus, laboratory and theoretical studies of which have elucidated many aspects of the general circulation of the atmospheres of the Earth and other planets. This paper outlines the findings of work on annulus convection produced by internal heating and mentions one particularly interesting possible application (Hide 1980) to the interpretation of long-lived anticyclonic eddies (including the Great Red Spot) seen in Jupiter's atmosphere.

2. Sloping convection in the laboratory

Laboratory experiments in thermal convection in a rotating fluid annulus which rotates about a vertical axis and is subject to axisymmetric applied differential heating were initiated by the writer over 30 years ago (for references see Hide and Mason 1975, Pfeffer, Buzyna and Kung 1980, and Tritton and Davies 1981). They show that when the rotation rate Ω exceeds a certain critical value Ω_R (which depends on the acceleration due to gravity, the shape and dimensions of the apparatus, the coefficients of thermal expansion, thermal conductivity and viscosity of the fluid and its mean density, and the distribution and intensity of the applied differential heating, see section 4 below) Coriolis forces inhibit overturning motions in meridian planes and promote a completely different kind of motion, which has been termed 'sloping convection'. The motion is then non-axisymmetric and largely confined to jet streams, with typical trajectories of individual fluid elements inclined at only very small but essentially non-zero angles to the horizontal. The kinetic energy of the non-axisymmetric flow derives from the interaction of slight upward and downward motions in these sloping trajectories with the potential energy field produced by the action of gravity on the density variations maintained by the applied differential heating. The kinetic energy of the motion is dissipated by friction arising in boundary layers on the walls of the container and in the main body of the fluid.

Provided that Ω, though greater than Ω_R, does not exceed a second critical value Ω_I (see section 4 below), the main features of the non-axisymmetric motion are characterized by great regularity. This regular flow is either steady (apart from a steady drift of the horizontal flow pattern relative to the walls of the apparatus) or it exhibits periodic 'vacillation' in the amplitude, shape and other characteristics. The number of 'waves' m around the annulus is not uniquely determined by the impressed conditions;

-3-

the flow is found to be ‘ ntransitive’ owing to the occurrence of what have come to be called ‘multiple equilibrium states’. But a quantity m, defined as the most likely value of m at a point in the region of parameter space occupied by the regular flow regime (where $\Omega_R < \Omega < \Omega_I$, see Fig. 1), tends to increase with increasing Ω, until at $\Omega = \Omega_I$ the quantity m has that value for which the azimuthal scale of the horizontal flow pattern (namely the mean circumference of the annulus divided by m) is about 1·5 times the radial scale. Then the motion undergoes a transition to the so-called regime of irregular flow, where $\Omega > \Omega_I$ in parameter space, which is an example of thermally driven ‘geostrophic turbulence’.

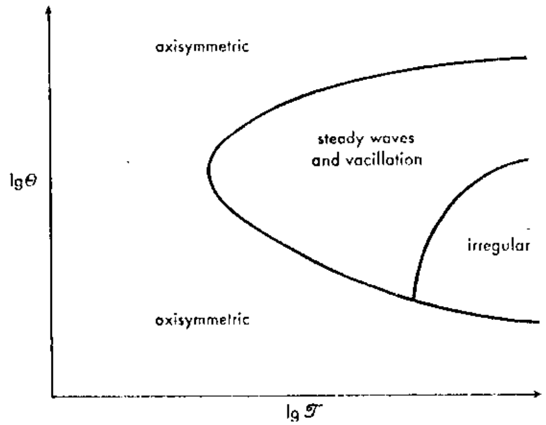

Figure 1. Schematic diagram illustrating the dependence of the mode of free thermal convection in a rotating fluid annulus under axisymmetric boundary conditions on the two dimensionless parameters found to specify the system, Θ and $\mathcal{T}$ (see equations (12) and (13)).

Many laboratory studies of various aspects of sloping convection have now been carried out. These include measurements of heat transfer, flow structure and regime transitions over a wide range of mechanical and thermal boundary conditions. Numerical studies are playing an increasingly important role in this work, and significant if more limited analytical studies have been made based on the essentially non-linear governing mathematical equations.

These equations are the equations of motion (2), together with the equations of continuity and state for a liquid, respectively

$$\nabla . u = 0 \qquad \ldots \qquad (3)$$

and

$$\rho = \rho_0 \{1 - \alpha(T - T_0)\} \qquad \ldots \qquad (4)$$

-4-

where T denotes temperature, α denotes thermal coefficient of cubical expansion and ρ_0 is the density at the reference temperature T_0, and the equation of heat transfer,

$$\frac{\partial T}{\partial t} + (u . \nabla)T = \kappa \nabla^2 T + q \qquad \ldots \qquad (5)$$

where κ is the thermal diffusivity (equal to the thermal conductivity divided by the product of ρ and the specific heat capacity c) and $q\rho c$ is the rate of diabatic heating per unit volume. Across any cylindrical vertical surface r = a constant, where (r, ϕ, z) are cylindrical polar coordinates of a general point, $r = 0$ being the rotation axis (see Fig. 2), and the rate of heat transfer is given by

$$H(r,t) = \int_0^d \int_0^{2\pi} \rho c \left(\kappa \frac{\partial T}{\partial r} + u_r T \right) r \, d\phi \, dz \qquad \ldots \qquad (6)$$

where the fluid extends in the axial direction from $z = 0$ to $z = d$. It is important to notice that the geostrophic contribution to the advective heat flow term on the right-hand side of equation (6) would vanish if the flow were axisymmetric, since by equation (1) u_r, the r component of $u = (u_r, u_\phi, u_z)$, satisfies $u_r \doteqdot (2\rho\Omega r)^{-1} \partial p/\partial\phi$. This result points to the *raison d'être* of the non-axisymmetric regime of flow found when $\Omega > \Omega_R$; geostrophic flow cannot convey heat perpendicularly to the axis of rotation unless it is non-axisymmetric!

The boundary conditions on u under which equations (2), (3), (4) and (5) must be satisfied are that $u = 0$ at a rigid bounding surface and that the stress should vanish at a free surface. The thermal boundary conditions require continuity of heat flow which, at a bounding surface, is purely conductive and proportional to $\kappa \nabla T$. When the boundary conditions on the side-walls at $r = r^*$, where $r^* = a$ or b (say, with $b > a$, see section 4 below), are combined with the geostrophic relationship given by equation

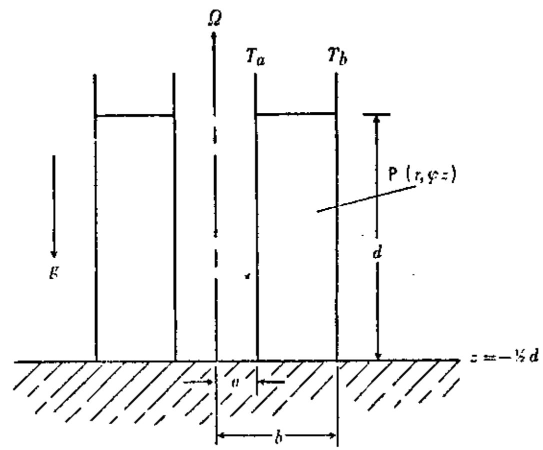

Figure 2. Schematic diagram of a rotating fluid annulus subject to a horizontal temperature gradient. (See Hide 1958 or Hide and Mason 1975 for further details.)

(1) and used in conjunction with the standard relationship for the radial flow in the Ekman boundary layers on $z = 0$ and $z = d$ to evaluate the radial heat flow at $r = r^*$ (see equation (6)), it is found (see Hide and Mason 1970) that:

$$H(r^*,t) \doteqdot -\left(\frac{\nu}{\Omega}\right)^{\frac{1}{2}}\left\{\bar{T}(r^*,d,t) - \bar{T}(r^*,0,t)\right\}\left\{\Gamma(r^*,d,t) - \Gamma(r^*,0,t)\right\}. \quad .. \quad .. \quad (7)$$

Here

$$\bar{T}(r^*,z,t) = \frac{1}{2\pi}\int_0^{2\pi} T(r^*,\phi,z,t)\mathrm{d}\phi \quad .. \quad .. \quad .. \quad .. \quad .. \quad (8)$$

and

$$\Gamma(r^*,z,t) = \int_0^{2\pi} U_\phi(r^*,\phi,z,t)r\,\mathrm{d}\phi, \quad .. \quad .. \quad .. \quad .. \quad .. \quad (9)$$

where $U_\phi(r^*,\phi,z,t)$ is the value of u_ϕ evaluated just outside the viscous boundary layer on $r = a$ or $r = b$, as the case may be. Now it may be shown that $\bar{T}(r^*,d,t) > \bar{T}(r^*,0,t)$ (when $\alpha > 0$, see equation (4)) and that either $\Gamma(r^*,0,t) = -\Gamma(r^*,d,\cdot)$ or $|\Gamma(r^*,0,t)| \leqslant |\Gamma(r^*,d,t)|$, according as the upper surface is in contact with a rigid lid or is free. Hence,

$$H(r^*,t) = (\text{negative definite quantity}) \times \Gamma(r^*,d,t). \quad .. \quad .. \quad .. \quad (10)$$

This relationship between the heat flow at a side-wall and the line integral of the tangential velocity near the side-wall embodies the arguments used by Hide (1958) to provide a general interpretation of the upper-level flow pattern in the case when $q = 0$ everywhere (see equation (5)), heat being introduced into the system via one of the side-walls and removed via the other side-wall. The corresponding impressed radial temperature gradient has the same sign at all values of r and the upper-level pattern of motion in the regular flow regime consists of a single jet stream meandering in a wavy pattern between the bounding cylinders, with a positive (i.e. 'westerly') azimuthal component when heat enters via the outer side-wall and leaves via the inner side-wall (so that the impressed radial temperature gradient is positive) and a negative ('easterly') component when the radial heat transfer is in the opposite direction, from the inner to the outer cylinder (see Figs 3(a) and 3(b)).

As a further test of equation (10) Hide and Mason (1970) carried out experiments using internal heating, so that the term q in equation (5) is not equal to zero. This was done by passing an alternating electric current through the fluid. Heat could be removed via the inner side-wall, the outer side-wall or both side-walls. The observed upper-surface flow patterns (see Fig. 4) were found to be in good agreement with predictions for these three cases made on the basis of equation (10) (see Figs 3(c), (d) and (e)). In the cases where heat is removed via one side-wall only, $H(r^*,t)$ vanishes at the other side-wall and by equation (10), the quantity $\Gamma(r^*,d,t)$ must also vanish. For this to happen, $U_\phi(r^*,\phi,d,t)$ will be positive at some values of ϕ and negative at others (or zero at all values of ϕ, as in the axisymmetric regime that occurs when $\Omega < \Omega_R$). Figs 3(c) and (d) show how this requirement can be satisfied by adding closed eddies to the wavy pattern found in the cases when $q = 0$ (cf. Figs 3(a) and (b)).

The most striking case of all studied in the experiments is the one illustrated by Fig. 3(e). Then, heat is removed via both side-walls, implying that the impressed radial temperature gradient changes sign near mid-radius. The corresponding upper-level flow consists of several separate closed eddies each circulating anticyclonically, in accordance with equation (10) with the horizontal flow confined to a narrow jet stream at the periphery of each eddy (see Fig. 4(e)).

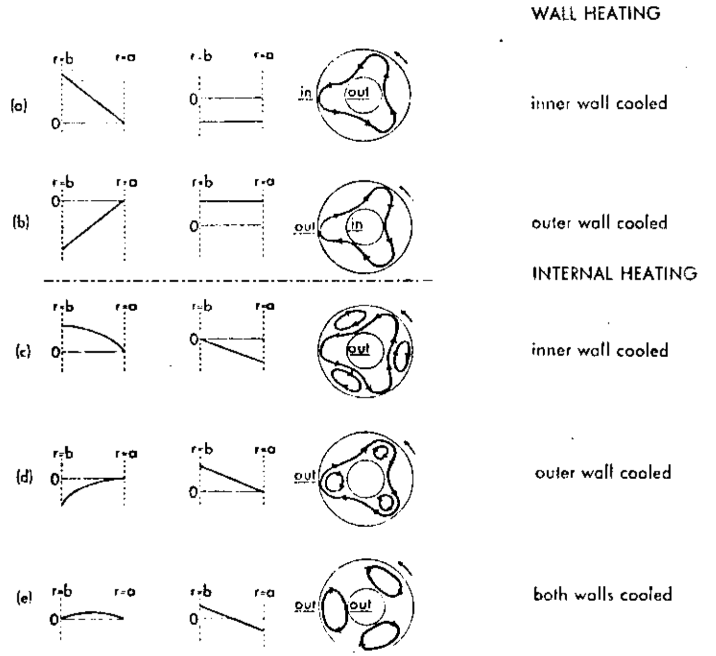

Figure 3. Schematic illustrations of the radial variation of the impressed temperature (left column), of the radial variation of the impressed radial temperature gradient (middle column), and of the corresponding upper-surface relative flow pattern in the regular regime of thermal convection in a rotating fluid annulus (right column), as predicted on the basis of equation (10). (See Hide and Mason 1970 for further details.)

3. Atmospheric flows

The meandering jet streams within which the upper-level tropospheric air flow is mainly concentrated in the Earth's atmosphere are manifestations of sloping convection produced by differential solar heating, which maintains a systematic temperature contrast between tropical and polar regions in each hemisphere. These atmospheric motions are much less regular than those depicted in Figs 3(a), 3(c) and 4(a) (cf. Fig. 5), presumably because the Earth's angular speed of rotation exceeds the critical value Ω_1, although horizontal variations of surface conditions introduce complications which are not yet fully understood.

The atmosphere of the planet Jupiter is heated from below at about the same rate as its upper reaches are heated by solar radiation. Unlike the terrestrial case (where non-solar atmospheric heating is utterly negligible), north–south temperature gradients in Jupiter's atmosphere change sign several times between equator and pole and there is no evidence of any significant systematic temperature contrast

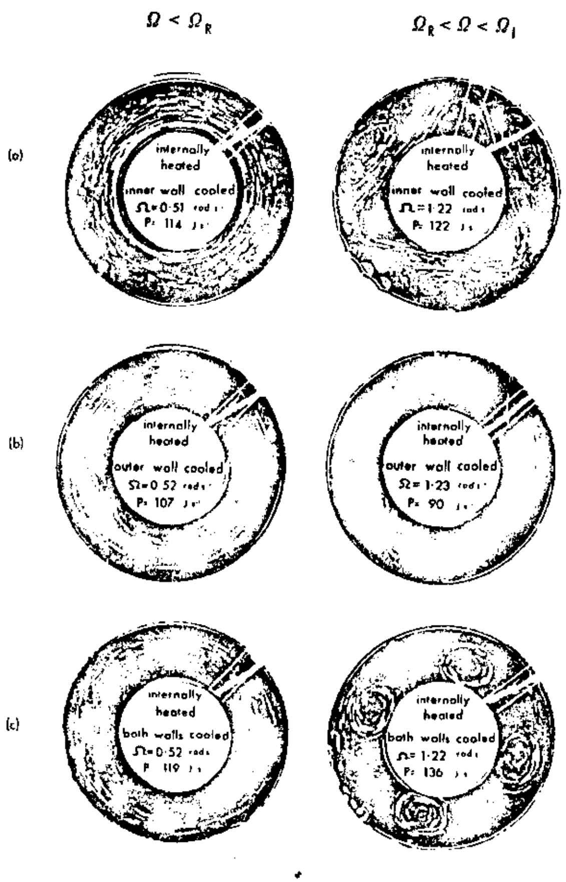

Figure 4. Streak photographs illustrating top-surface flow patterns of thermal convection in a rotating fluid annulus subject to internal heating in the axisymmetric regime (when $\Omega < \Omega_R$, see left column) and regular non-axisymmetric regime (when $\Omega_R < \Omega < \Omega_I$, see right column). They show the dependence of the general characteristics of the flow pattern on the way heat is removed from the system and confirm predictions based on equation (10). The cases (a), (b) and (c) correspond to cases (c), (d) and (e) respectively in Fig. 3. In the most striking case of all (see Figs 3(e) and 4(c)) sloping convection takes the form of closed anticyclonic eddies with the main motion concentrated in a jet stream at the periphery of each eddy. (See Hide and Mason 1970 for further details.)

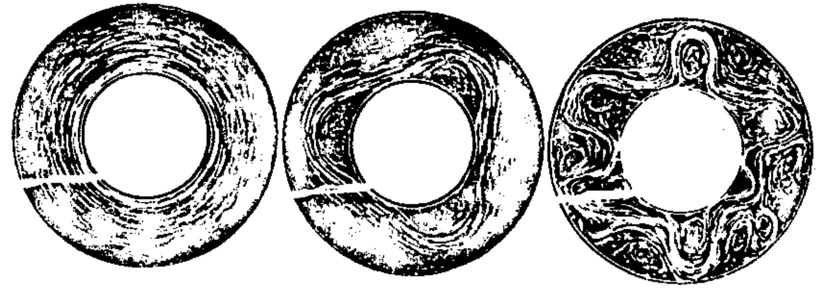

(I) symmetric (Ω = 0·341 rad s^{-1}) (II) steady waves (Ω = 1·19 rad s^{-1}) (III) irregular (Ω = 5·02 rad s^{-1})

Figure 5. Streak photographs giving one example of each of the main modes of thermal convection in a rotating fluid annulus subject to a radial temperature field of the form given by equation (11), namely (I) axisymmetric flow, (II) regular (steady) non-axisymmetric flow, and (III) irregular non-axisymmetric flow.

between equatorial and polar regions (for references see Ingersoll, Dobrovolskis and Jakosky 1979). There are abundant observations of Jovian atmospheric motions at the upper-cloud level, some of which go back many decades and even longer, and the Pioneer and Voyager space probes have added further details (see Peek 1958, Smith and Hunt 1976, NASA 1979 and Mitchell *et al.* 1981). Our knowledge of what goes on below the cloud level is meagre and this produces difficulties with the interpretation of observations of upper-level atmospheric motions. Indeed, it has been argued elsewhere that the main task of the 'Jovian meteorologist' should perhaps be to use these observations to improve our knowledge of the vertical structure of the planet (see e.g. Hide 1981).

But here is not the place to discuss these observations and review the many interesting though largely controversial issues being debated by those of us who take an interest in the interpretation of the observations in terms of basic dynamical processes. There is, however, one striking phenomenon upon which laboratory experiments on sloping convection in a fluid annulus subject to internal heating might have some bearing. The highly stable closed anticyclonic eddies with the main motion concentrated in a jet stream at the periphery of each eddy that are depicted in Figs 3(e) and 4(c) are remarkably similar dynamically to the long-lived eddies to be seen in Jupiter's atmosphere in the southern hemisphere. The largest, oldest and most conspicuous of these is the Great Red Spot in the South Tropical Zone which may be at least 300 years old. Next in size and age are the three White Ovals that formed in 1939 at the boundary between the South Temperate Belt and the South Temperate Zone, apparently as the residue of the highly irregular South Tropical Disturbance that was first seen in 1901. The smallest of the long-lived eddies are clearly seen in the magnificent Voyager pictures (NASA 1979) as about a dozen oval markings somewhat closer to the pole. The motion in each of these Jovian eddies is anticyclonic and largely confined to a narrow region at the edge of the eddy. It is tempting therefore to suppose (Hide 1980) that the eddies are manifestations of sloping convection in Jupiter's atmosphere, implying that they derive their kinetic energy directly from the potential energy due to the action of gravity on density variations produced by internal and solar heating and that they transport heat from the interior to the edges of the latitudinal bands in which they arise. (See Plate I.)

Preliminary calculations indicate that there is nothing unreasonable about this hypothesis so far as its implications for the vertical structure and other properties of Jupiter's atmosphere are concerned, but a detailed examination of these implications and a critical comparison of the hypothesis with other proposals as to the nature of the long-lived anticyclonic eddies will have to be considered elsewhere. The hypothesis raises a number of fluid-dynamical questions to be resolved by further laboratory and numerical work and some of this is now in hand. Amongst these questions is that of the instability of the strongly sheared flow in the jet stream itself. Experiments with a wall-heated annulus (Hide 1958) provide some evidence that when viscous effects are sufficiently small the jet stream develops local instabilities on one side but not on the other. Pictures of Jupiter show highly irregular flow on a comparatively small scale just outside the Great Red Spot (and the other long-lived eddies), but not on the inside. It will be important to establish by experiment and theory (cf. Narasimha 1980) whether this highly irregular flow arises as a result of a 'one-sided' instability of the jet stream at the edge of the main eddy.

4. Appendix: Regimes of thermal convection in a rotating fluid annulus

The simplest system in which controlled and reproducible experiments on sloping convection have been carried out is the annular apparatus illustrated in Fig. 2 when there are no internal sources of heat (i.e. $q = 0$, see equation (5)) but the bounding cylindrical side-walls in $r = a$ and $r = b$ are maintained at different temperatures T_a and T_b respectively, so that the impressed temperature field satisfies

$$T_i = \{T_b \ln(r/a) - T_a \ln(r/b)\}/\ln(b/a), \qquad (11)$$

which simplifies to $T_i = \frac{1}{2}(T_b + T_a) + (T_b - T_a)\{r - \frac{1}{2}(a+b)\}/(b-a)$ when $(b-a) \ll \frac{1}{2}(b+a)$. Accurate determinations of the principal spatial and temporal characteristics of the fields of temperature and flow velocity over a wide range of precisely specified and carefully controlled experimental conditions led to the discovery of several fundamentally different free types of flow, only one of which is symmetrical about the axis of rotation (see Figs 5 and 6). The general character of the flow evidently depends largely on the values of certain external dimensionless parameters,

$$\Theta \equiv gd\Delta\rho/\bar{\rho}\Omega^2(b-a)^2 \qquad (12)$$

and

$$\mathscr{T} \equiv 4\Omega^2 L^4/\nu^2 \qquad (13)$$

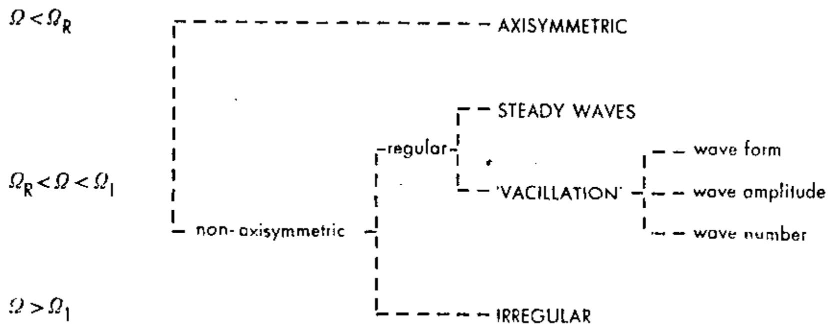

Figure 6. Broad classification of modes of free thermal convection in a rotating fluid annulus under axisymmetric boundary conditions. (See Hide 1958 or Hide and Mason 1975 for further details.)

Here g denotes the acceleration due to gravity (which is typically very much greater than $\Omega^2 b$), d is the depth of the liquid in the annular container, $\Delta\rho$ is the density contrast associated with the impressed temperature difference, i.e. $|\rho(T_a) - \rho(T_b)|$, $\bar{\rho}$ is the mean density, Ω is the angular speed of rotation of the apparatus about a vertical axis, ν is the kinematic viscosity and L, which has the dimensions of a length, is equal to $(b-a)^{5/4}/d^{1/4}$ over a wide range of conditions.

When $\mathscr{T}$ is less than a certain critical value of about 2×10^5 (see Fig. 1), viscosity ensures that the motion is essentially symmetrical about the axis of rotation for all values of Θ. However, when $\mathscr{T}$ exceeds this critical value there exists a range of Θ within which highly non-axisymmetric sloping convection occurs. These non-axisymmetric motions are either regular or irregular (see Fig. 5) depending on the values of Θ and $\mathscr{T}$. The regular flows often exhibit periodic 'vacillation' in amplitude, shape or wavenumber, but under certain conditions these periodic variations are so slight that, apart from a steady drift of the wavy pattern relative to the apparatus, the flow is virtually steady. In sharp contrast to this behaviour, the irregular flows exhibit complicated aperiodic fluctuations in both space and time.

Consider an experiment in which all the impressed conditions are kept fixed except Ω, which is increased in steps from low values to high values. This can be represented by a series of points on a straight line inclined at 45° to the $\mathscr{T}$ and Θ axes in the regime diagram of Fig. 1, moving from the upper left part of the diagram to the lower right. The critical value Ω_R of Ω corresponds to the point where the transition from axisymmetric to regular non-axisymmetric flow occurs and the critical value Ω_I to the point where the transition from regular to irregular non-axisymmetric flow occurs.

References

Hide, R. 1958 An experimental study of thermal convection in a rotating liquid. *Philos Trans R Soc, London*, A, 250, 441–478. (For further details see Hide, R., Ph.D. dissertation, Cambridge University, 1953.)

Hide, R. 1980 Jupiter and Saturn: giant magnetic rotating fluid planets. *Observatory*, 100, 182–193.

Hide, R. 1981 On the rotation of Jupiter. *Geophys J R Astron Soc*, 64, 283–289.

Hide, R. and Mason, P. J. 1970 Baroclinic waves in a rotating fluid subject to internal heating. *Philos Trans R Soc, London*, A, 268, 201–232.

Hide, R. and Mason, P. J. 1975 Sloping convection in a rotating fluid. *Adv Phys*, 24, 47–100.

Ingersoll, A. P., Dobrovolskis, A. R. and Jakosky, B. M. 1979 Planetary atmospheres. *Rev Geophys Space Phys*, 17, 1722–1735.

Mitchell, J. L., Beebe, R. F., Ingersoll, A. P. and Garneau, G. W. 1981 Flow fields within Jupiter's Great Red Spot and White Oval BC. *J Geophys Res* (in press).

Narasimha, R. 1980 The possible influence of curvature and rotation on ocean currents. *Proc Indian Acad Sci (Earth Planet Sci)*, 89, 267–275.

NASA 1979 Voyager encounters Jupiter. Washington, D.C., National Aeronautics and Space Administration.

Peek, B. M. 1958 The planet Jupiter. London, Faber.

Pfeffer, R. L., Buzyna, G. and Kung, R. 1980 Time-dependent modes of behaviour of thermally driven rotating fluids. *J Atmos Sci*, 37, 2129–2149.

Smith, B. A. and Hunt, G. E. 1976 Motions and morphology of clouds in the atmosphere of Jupiter. *In* Gehrels, T. (ed.), Jupiter: studies of the interior, atmosphere, magnetosphere and satellites. Tucson, University of Arizona Press.

Tritton, D. J. and Davies, P. A. 1981 Instabilities in geophysical fluid dynamics. *In* Swinney, H. L. and Gollub, J. P. (eds), Hydrodynamic instabilities and the transition to turbulence. Berlin, Heidelberg, New York, Springer-Verlag.

Printed in England for Her Majesty's Stationery Office by Heffers Printers Ltd, Cambridge

To face page 344

Plate I. Long-lived anticyclonic eddies in Jupiter's atmosphere, namely the Great Red Spot (which is about 20 000 km long) and one of the three White Ovals. The arrows indicate the sense of relative motion. The speeds (as determined by Dr R. F. Beebe of the New Mexico State University) are given in kilometres per hour; for comparison note that points on Jupiter's equator rotate at about 35 000 km per hour. (See NASA 1979 for further Voyager pictures of Jupiter).